Ocean–Atmosphere Influences on Low-Frequency Warm-Season Drought Variability in the Gulf Coast and Southeastern United States

JASON T. ORTEGREN

Department of Environmental Studies, University of West Florida, Pensacola, Florida

PAUL A. KNAPP, JUSTIN T. MAXWELL, AND WILLIAM P. TYMINSKI

Department of Geography, University of North Carolina at Greensboro, Greensboro, North Carolina

PETER T. SOULÉ

Department of Geography and Planning, Appalachian State University, Boone, North Carolina

(Manuscript received 26 May 2010, in final form 1 October 2010)

ABSTRACT

From the 344 state climate divisions in the conterminous United States, nine distinct regions of warm-season drought variability are identified using principal component analysis. The drought metric used is the Palmer hydrological drought index for the period 1895–2008. The focus of this paper is multidecadal drought variability in the Southeast (SEUS) and eastern Gulf South (EGS) regions of the United States, areas in which the low-frequency forcing mechanisms of warm-season drought are still poorly understood. Low-frequency drought variability in the SEUS and EGS is associated with smoothed indexed time series of major ocean–atmosphere circulation features, including two indices of spatiotemporal variability in the North Atlantic subtropical anticyclone (Bermuda high). Long-term warm-season drought conditions are significantly out of phase between the two regions. Multidecadal regimes of above- and below-average moisture in the SEUS and EGS are closely associated with slow variability in sea surface temperatures in the North Atlantic Ocean and with the summer mean position and mean strength of the Bermuda high. Multivariate linear regression indicates that 82%–92% of the low-frequency variability in warm-season moisture is explained by two of the three leading principal components of low-frequency variability in the climate indices. The findings are important for water resource managers and water-intensive industries in the SEUS and EGS. The associations identified in the paper are valuable for enhanced drought preparedness and forecasting in the study area and potentially for global models of coupled ocean–atmosphere variability.

1. Introduction

Worldwide, drought is the most common natural hazard (Hayes et al. 2004). In recent decades, notable advances have been made in understanding regional drought patterns and, in many places, the causes of persistent droughts. For the period covered by reliable instrumental meteorological observations (1895–present), spatiotemporal patterns of drought in the United States have received much attention (e.g., Soulé 1992; Henderson and Vega 1996; Knapp et al. 2002; Kangas and Brown

2007). Further, proxy records of paleoclimatic variability (primarily tree rings) have been used to reconstruct multicentury drought variability over much of North America (e.g., Stahle et al. 1988, 1998, 2007; Stahle and Cleaveland 1988; Cook and Krusic 2004; Herweijer et al. 2007). A number of studies have specifically addressed historic and contemporary drought variability in the Southeast and Gulf South regions as well (Stahle and Cleaveland 1988, 1992, 1994; Stahle et al. 1988; Seager et al. 2009). One notable feature of drought variability in these regions is the persistence of low-frequency variability (~30-yr regime-like behavior) in growing-season moisture conditions, with multidecadal periods of above- and below-average wetness (Stahle et al. 1988; Stahle and Cleaveland 1992; Cook and Krusic 2004; J. T. Ortegren 2008, unpublished manuscript). A second

Corresponding author address: J. T. Ortegren, Dept. of Environmental Studies, University of West Florida, 11000 University Pkwy., Pensacola, FL 32514.
E-mail: jortegren@uwf.edu

feature of drought variability in these regions is the relative absence of severe sustained (e.g., decadal-scale) continuous droughts during previous centuries (e.g., Stahle and Cleaveland 1992; Cook and Krusic 2004).

Because drought implies prolonged precipitation and soil moisture deficits, it is often modulated by low-frequency ocean–atmosphere oscillations (Mo et al. 2009). Previous studies have examined and/or modeled ocean–atmosphere influences on North American drought, including SST anomalies in the tropical Pacific Ocean and the subtropical Atlantic Ocean (Hoerling and Kumar 2003; Seager et al. 2005; Sutton and Hodson 2005). Ocean–atmosphere influences on drought in the western United States have been discussed by several authors (e.g., Schubert et al. 2004; Seager et al. 2005; Herweijer et al. 2007; Stahle et al. 2007). For the Southeast, moisture conditions during the winter half-year are principally associated with subdecadal variability in the time series index of the El Niño–Southern Oscillation (ENSO; Cordery and McCall 2000; Rogers and Coleman 2003; Seager et al. 2009).

Low-frequency drivers of persistent warm-season droughts in the Southeast are not as well understood, although possible causes have been discussed (Stahle and Cleaveland 1988, 1992; Trenberth et al. 1988; Seager et al. 2009).

The difficulty of short-term drought forecasting in the Southeast using tropical Pacific SST anomalies has been demonstrated by Seager et al. (2009). The region tends to experience wetter (drier) winters associated with El Niño (La Niña) conditions, but this relationship is nonstationary both temporally and spatially (McCabe et al. 2004; Seager et al. 2009). Short-term (i.e., interannual) summer half-year drought variability is the result of internal atmospheric behavior, with no significant influence from the tropical Pacific (Seager et al. 2009). Moreover, they conclude that summer half-year drought conditions are essentially unpredictable (Seager et al. 2009).

However, low-frequency warm-season drought patterns in the Southeast may be predictable owing to linkages with ocean–atmosphere oscillations in the North Atlantic (e.g., Enfield et al. 2001; McCabe et al. 2004). This is important because, despite the relatively infrequent occurrence of decadal-scale drought, much of the Southeast is currently susceptible to severe municipal and agricultural water resource shortages that result from droughts lasting only one or two years. Continued population growth only increases these concerns (J. T. Ortegren 2008, unpublished manuscript; Seager et al. 2009).

Previous investigators have suggested the possibility of coupled ocean–atmosphere behavior in the Atlantic basin that may be an important component of multidecadal climate variability at both regional and global scales (Marshall et al. 2001; Sutton and Hodson 2005; McCabe and Palecki 2006). Among the circulation features with reported warm-season teleconnections to drought in the Southeast are the Atlantic multidecadal oscillation (AMO; Enfield et al. 2001; McCabe et al. 2004; Knight et al. 2006), and, in ways less understood, the Pacific decadal oscillation (PDO; McCabe et al. 2004). The AMO index is strongly inversely correlated ($r = -0.72$, $p < 0.001$) with the 30-yr moving average of summer drought variability in the Piedmont region of the Southeast (J. T. Ortegren 2008, unpublished manuscript). Thus, multidecadal regimes of above-average warm-season moisture are associated with cool phases of the AMO, and warm phases are associated with drier-than-average regimes (McCabe et al. 2004; J. T. Ortegren 2008, unpublished manuscript).

Long-term variability in the semipermanent North Atlantic subtropical anticyclone (hereinafter the Bermuda high) also appears to be linked to warm-season moisture variability in the Southeast (Stahle and Cleaveland 1992; Henderson and Vega 1996; Davis et al. 1997; Diem 2006). During the instrumental period, the Bermuda high has exhibited multidecadal variability in both mean location and mean central pressure (Sahsamanoglou 1990; Davis et al. 1997; Anchukaitis et al. 2006), with associated impacts on moisture advection into the Southeast and Gulf Coast regions. Keim (1997) provides a description of the basic dynamics behind the influence of the Bermuda high on low-level atmospheric stability and warm-season extreme rainfall events in the two regions.

Our primary objective is to examine long-term warm-season drought variability in the southeastern United States, including areas of the Gulf South, to determine if these regions are responding to coupled ocean–atmosphere variability in the Atlantic basin. We first examine the instrumental climate record (1895–2008) to quantitatively define the "Southeast" and "Gulf Coast" drought regions. We test the hypothesis that our study area is less susceptible to prolonged severe droughts than other regions of the conterminous United States, and we assess long-term associations between drought variability and a suite of time-series indexed oceanic and atmospheric forcing mechanisms with the goal of isolating teleconnective features that enhance our ability to predict and prepare for multidecadal changes in drought likelihood and intensity. Our specific objectives are to

1) quantitatively define homogeneous warm-season drought regions in the conterminous United States (i.e., in terms of warm-season drought variability, where are the Southeast and the Gulf South?);

2) evaluate regional susceptibility to severe, prolonged droughts during the instrumental period under the hypothesis that the Southeast and Gulf South are climatologically less prone to multiyear droughts than other regions of the United States; and

3) analyze ocean–atmosphere influences on long-term warm-season drought variability in the Southeast and eastern Gulf South to enhance the accuracy of baseline conditions used in seasonal drought forecasts.

2. Data

a. Drought data

We retrieved mean monthly values of the Palmer hydrological drought index (PHDI) for each of the 344 state climate divisions in the conterminous United States for the period 1895–2008 from the National Climatic Data Center (online at http://www7.ncdc.noaa.gov/CDO/CDODivisionalSelect.jsp#). The PHDI is similar to the better-known Palmer drought severity index but is formulated to respond more slowly to moisture changes, making it a more appropriate index of hydrological drought (i.e., water resource impacts) than of meteorological drought (Palmer 1965). Calculation of the PHDI includes moisture conditions in previous and successive months from the month of interest. For example, summer average PHDI includes information about the preceding spring and the following autumn (Soulé 1992; Kangas and Brown 2007). Because of this, we analyzed summer (June–August) average PHDI, which is a good indicator of water resource limitations in the summer half-year during which the causes of drought in the Southeast are less understood than during the winter half-year (e.g., Seager et al. 2009). The PHDI is commonly used in climatic studies and provides an excellent measure of moisture balance (e.g., Stahle et al. 1998).

b. Ocean–atmosphere data

We obtained monthly sea level pressure (SLP) data on a 5° latitude–longitude grid from the National Center for Atmospheric Research (NCAR) for the period 1900–2008 (online at http://dss.ucar.edu/datasets/ds010.1/). We selected SLP data from the Atlantic basin to create two atmospheric indexes: one to approximate the mean location of the west flank of the Bermuda high, and the other to track temporal variability in the mean central pressure of the Bermuda high. Additionally, we assembled monthly data for the period 1900–2008 for the following: 1) the AMO index [National Oceanic and Atmospheric Administration (NOAA); online at http://www.esrl.noaa.gov/psd/data/correlation/amon.us.long.data]; 2) the PDO index (University of Washington Joint

Institute for the Study of the Atmosphere and Ocean; online at http://jisao.washington.edu/pdo/PDO.latest); 3) the station-based North Atlantic Oscillation (NAO) index (NCAR Climate and Global Dynamics Climate Analysis Section; online at http://www.cgd.ucar.edu/cas/jhurrell/indices.data.html#naostatmon); 4) the Southern Oscillation index (SOI; Australian Government Bureau of Meteorology; online at http://www.bom.gov.au/climate/current/soihtm1.shtml); and 5) the ENSO index [National Aeronautics and Space Administration (NASA) Goddard Space Flight Center Global Change Master Directory; online at http://www.esrl.noaa.gov/psd/data/correlation/censo.long.data].

3. Methods

a. Drought regionalization

We used principal component analysis (PCA) to isolate the leading modes of warm-season drought (PHDI) variability in the 344 state climate divisions of the conterminous United States. We compared maximum factor loadings from the PCA with different numbers of factors retained and Varimax rotation to identify the number of principal components (PCs) of drought variability that reflected reasonably contiguous and logical regions (e.g., Horel 1981; Acker and Soulé 1995; Timilsena and Piechota 2008). We also collected the time series of factor (regression) scores for each PC extracted.

b. Definition of a sustained drought event

We defined a prolonged drought event as any period ≥3 consecutive years in which summer average PHDI was ≤−1. We presume that two consecutive years of mild or moderate drought conditions may result from internal climatic fluctuations or short-term (high frequency) teleconnective variability, rather than low-frequency large-scale climatic forcing. Droughts lasting three years or longer are more likely to be caused by synoptic conditions related to ocean–atmosphere interactions and embedded upper-troposphere patterns. While a PHDI value of −1 is nominally classified as "midrange," continuous periods below the long-term mean (i.e., negative PHDI) indicate the potential for substantial water resource impacts because of the cumulative effects of water deficiencies. Additionally, we found that a more stringent cutoff (e.g., PHDI ≤ −2) would exclude most climate divisions in the country, where no multiyear drought in the instrumental period persisted with this "moderate" (or worse) severity for three or more years. However, the droughts of the 1930s and 1950s in the Great Plains and the Southwest, respectively, were known to have extreme impacts, even though only a few scattered

Dust Bowl climate divisions would have qualified under a stricter definition of a multiyear drought event based on summer average PHDI. Thus, the selected threshold value is conservative enough to be a reliable indicator of cumulative moisture deficiency.

c. Drought susceptibility comparisons

We computed average drought length (consecutive warm seasons) and average drought severity (PHDI) for each climate division in each region according to our drought event definition. To assess combined length and severity characteristics of droughts between regions we calculated the product of average drought length and average drought severity. We averaged the results for each measure across all climate divisions in each region for comparison. We indexed the average length times average severity measure as a z score for each climate division in each region, and averaged these drought susceptibility index values across all climate divisions in each PC to facilitate regional comparison. Larger values indicate greater susceptibility to long, severe droughts.

d. Creation of atmospheric indices

To index annual variability in the mean summer location of the western flank of the Bermuda high, we employed a methodology similar to Stahle and Cleaveland (1992) and Katz et al. (2003). We used the grid point 35°N, 65°W to approximate the location of Bermuda, and the point 30°N, 90°W to represent New Orleans. The difference in mean summer SLP (Bermuda minus New Orleans) effectively approximates the location of southerly airflow in the western flank of the Bermuda high, with larger values indicating a more eastward location. The standardized time series of these differences we termed the Bermuda high index (BHI).

To assess the hydroclimatological impacts of temporal variability in the strength of the Bermuda high (i.e., the strength of southerly flow and vapor advection to the southeastern portion of the conterminous United States) we calculated mean central pressure during summer regardless of location. We recorded the maximum monthly SLP for June, July, and August for all grid points in the subtropical Atlantic between 20° and 50°N (inclusive) and between 80°W and 0° (inclusive). We standardized the time series of annual mean central pressure during summer to create the mean central pressure index (MCP).

e. Ocean–atmosphere analyses

To isolate the low-frequency circulation features that influence warm-season drought patterns, we smoothed the time series of PHDI factor scores for each PC using 10-, 15-, 20-, 25-, and 30-yr moving averages. We ran Pearson bivariate correlations between the smoothed

PHDI factor scores and similarly smoothed time series of the selected climate indices (AMO, BHI, MCP, PDO, ENSO, SOI, and NAO). Because of the serial correlation in smoothed series, traditional significance tests are unreliable. Therefore, throughout this study, when correlating smoothed series we estimated significance levels using a Monte Carlo simulation (e.g., McCabe et al. 2004). We report only those associations with estimated significance levels greater than 98% (i.e., $p < 0.02$).

We correlated the factor scores of interannual (and smoothed) PHDI variability from the Southeast (SEUS) and eastern Gulf South (EGS) against the interannual (and similarly smoothed) time series of the seven climate indices (summer averages) included in the study. To reduce the climate index data to fundamental modes of low-frequency variability, we analyzed the 30-yr smoothed time series of ocean–atmosphere indices using PCA. For this analysis we did not include the ENSO index, which exhibited no significant correlations with factor scores of warm-season drought variability in our study area. We retained the time series of factor scores from each climate index PC for comparison with the factor scores of PHDI variability.

f. Predictability analysis

We created a multivariate linear regression model to assess the proportional and combined influences of separate large-scale forcing mechanisms on low-frequency drought in the SEUS and EGS. We used the factor scores of variability from the PCA of ocean–atmosphere indices as regressor variables to predict low-frequency PHDI variability in the two regions. To evaluate the utility of the model, we performed a split-period model calibration and verification procedure commonly employed in dendrochronological research (e.g., Fritts 1976). For both the SEUS and EGS, we used the first half (1929–67) of the data series to construct a regression model and obtain model coefficients for the predictor variables. With this model, we estimated the second half (1968–2008) of the drought variability time series, the observed values of which are independent (i.e., were not used to construct the model). The predictive accuracy of the model was assessed using the Pearson correlation coefficient (r) between estimated and observed (independent) values as well as the reduction of error (RE) statistic (e.g., Fritts 1976).

4. Results and discussion

a. Drought regionalization

The results of rotated PCA with different numbers of PCs extracted indicated that the regions stabilized
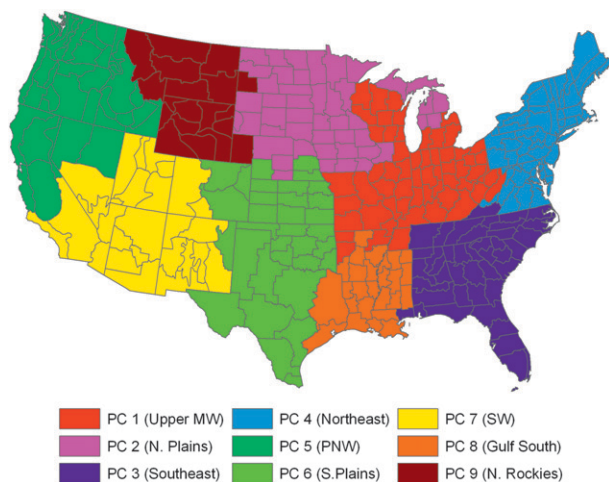
FIG. 1. Drought regionalization based on maximum factor loading scores for the first nine rotated principal components of summer average PHDI variability in the conterminous United States, 1895–2008.

(showed minimal splintering) and were physically coherent when the first nine PCs were retained. By assigning each climate division to a region (PC) based on maximum factor loadings, we defined nine distinct regions of homogeneity in summer average PHDI variability in the contiguous United States for the period of record (Fig. 1). These nine PCs explained 68.5% of the variance in climate division summer average PHDI during the period 1895–2008. We assigned colloquial region names to the nine regions for ease of reference (Table 1).

While the PCA results strongly suggested that the first nine rotated PCs were optimal for isolating clusters of similar drought variability, a total of 17 (4.9%) of the state climate divisions still were not smoothly contiguous (i.e., showed some splintering into other regions). In nearly all cases the ''splinter'' divisions exhibited significant ($p < 0.001$) correlations with the time series of factor scores from the surrounding PC (region). This indicates that ''splinter'' divisions may represent natural transition zones of drought variability, exhibiting temporal patterns of drought that reflect elements of the region to which they were assigned, as well as elements

of the region that surrounds them. Only five climate divisions, representing 1.5% of the total, exhibited splintering in the Southeast and Gulf South regions that are the focus of this study. To assure regional contiguity and minimize noise in the results, we assigned each splinter division to the region surrounding it.

b. Regional susceptibility to severe prolonged drought

Our analysis of overall drought susceptibility, as measured by indexing regional average drought severity times regional average drought length, indicated that the regions with the lowest susceptibility to severe prolonged drought during 1895–2008 were the EGS and SEUS (Table 1). These results are in general agreement with Stahle and Cleaveland (1992), Cook and Krusic (2004), and J. T. Ortegren (2008, unpublished manuscript). The Northern Rockies (NROK) and Southern Plains (SPLN) were most susceptible during the same period. The EGS experienced the lowest average drought length, lowest average severity, and the lowest susceptibility index value, followed closely by the SEUS in each category. The NROK experienced the ''worst'' drought conditions according to these same measures, followed by the SPLN. Because of our focus on low-frequency drought patterns in the Southeast and Gulf South, in this paper we do not present analyses of drought variability in the other seven regions.

c. Low-frequency influences on warm-season drought

Although longer smoothing windows did not always produce higher correlations between series, the multidecadal patterns of PHDI and climate index variability seemed to be best reflected in the 20–30-yr moving-average time series. Also, existing evidence indicates roughly 30-yr regimes of moisture variability in the study area (e.g., Stahle and Cleaveland 1992). All subsequent analyses were conducted using the 30-yr smoothed series of each variable. The ENSO index was not significantly correlated with warm-season drought variability in the SEUS or in the EGS at any time scale and was not included in further analyses. The SOI was included and is expected to capture much of the ENSO variability

TABLE 1. Regional average warm-season drought characteristics, 1895–2008. A drought event is defined as three or more consecutive summers with average PHDI ≤ -1.

Measure	Upper Midwest	Northern Plains	Southeast	Northeast	Pacific Northwest	Southern Plains	Southwest	Eastern Gulf South	Northern Rockies
Avg length (consecutive summers)	3.79	4.78	3.81	4.68	4.45	4.76	4.56	3.69	4.81
Avg severity (PHDI)	−2.54	−3.05	−2.39	−2.34	−2.73	−3.15	−3.17	−2.25	−3.21
Avg length × avg severity	−9.67	−14.57	−9.13	−11.16	−12.25	−15.16	−14.62	−8.28	−15.64
Drought susceptibility index	0.79	1.18	0.74	0.91	1.00	1.23	1.19	0.67	1.27

TABLE 2. Significant ($p < 0.02$ as estimated by Monte Carlo significance tests) bivariate correlation coefficients between 30-yr smoothed climate index time series and 30-yr smoothed PHDI variability in the SEUS and EGS.

	AMO	BHI	MCP	PDO	SOI	NAO
AMO	—	−0.82	−0.34			
BHI		—	0.40			
MCP			—		0.30	0.42
PDO				—	−0.83	
SOI					—	0.36
NAO						—
—	—	—	—	—	—	—
SEUS	−0.72	0.62	−0.34			−0.42
EGS	0.79	−0.81	−0.65			

FIG. 2. Smoothed time-series plots of the AMO, BHI, and warm-season drought variability in the SEUS.

(interannual correlation between SOI and ENSO: $r = −0.898$, $p < 0.001$).

Low-frequency SEUS drought variability (smoothed PC factor scores) is significantly associated with low-frequency variability in the AMO, BHI, NAO, and MCP (Table 2; Figs. 2 and 3). The AMO and BHI are strongly negatively associated, indicating that warm (cool) phases of the AMO tend to coincide with multidecadal periods of anomalous westward (eastward) migration of the Bermuda high during summer and are associated with dry (wet) summer regimes in the SEUS.

Low-frequency EGS drought variability is significantly associated with low-frequency variability in the AMO, BHI, and MCP (Table 2; Figs. 4 and 5). The EGS associations with AMO and BHI are of opposite sign to those in the SEUS. However, both the EGS and SEUS are weakly negatively associated with MCP. This finding is counter to previous hypotheses that the westward displacement of the Bermuda high resulted from expansion of the anticyclone, rather than migration (e.g., Keim 1997). Both the SEUS and the EGS are drier under the influence of stronger southerly airflow induced by a steeper horizontal pressure gradient in the Atlantic Basin, implying that these conditions may not necessarily facilitate enhanced moisture conditions in the study areas.

The opposite response in the EGS and SEUS to variability in the AMO and BHI indicates the possibility that long-term warm-season moisture conditions may be out of phase in the two regions. The 30-yr smoothed time series of drought variability between the EGS and the SEUS are significantly negatively correlated ($r = −0.37$). This negative association is stronger at the 20- and 25-yr smoothing lengths ($r = −0.451$ for both lengths). These results indicate that slow variations in the AMO, BHI, and MCP are the principal drivers of multidecadal warm-season drought variability in the SEUS and the EGS but with opposite responses between the two regions.
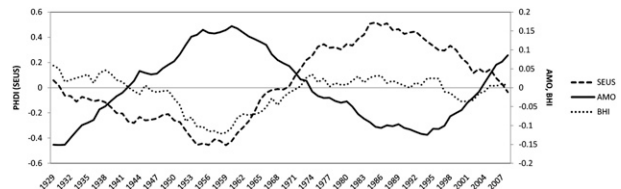
Because the SEUS and EGS associations with MCP are of the same sign, the out-of-phase moisture conditions between the two regions are primarily explained by the AMO and BHI.

d. Ocean–atmosphere interactions

Multidecadal regimes of above- (below) average warm-season moisture in the SEUS (EGS) are associated with cool phases of the AMO, during which the western flank of the Bermuda high in summer is typically displaced eastward of its mean position. These periods also correspond to regimes of enhanced strength (i.e., central pressure) of anticyclonic airflow around the Bermuda high. The period from the 1960s to early 1990s is an example of a period during which these circumstances dominated.

The negative association between the MCP and AMO is logical, as reduced SSTs in the Atlantic Ocean (AMO−) should be associated with enhanced subsidence and higher surface pressure, particularly during the warm season when the horizontal surface temperature gradient between the Atlantic and the surrounding continents is greatest (e.g., Keim 1997). Further, cool SSTs in the tropical North Atlantic are associated with strong trade winds above them and possible intensification of the Hadley circulation (Marshall et al. 2001). An increase in central pressure of the Bermuda high implies enhanced southerly airflow and moisture advection on the western flank of the anticyclone, which is typically focused on the mid-Atlantic coast of the SEUS during cool AMO phases.

Conversely, multidecadal regimes of below- (above) average warm-season moisture in the SEUS (EGS) are associated with warm phases of the AMO, westward
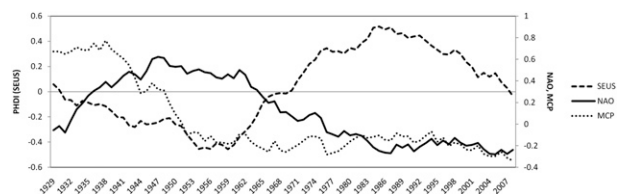

FIG. 3. As in Fig. 2, but for the NAO, MCP, and warm-season drought variability.
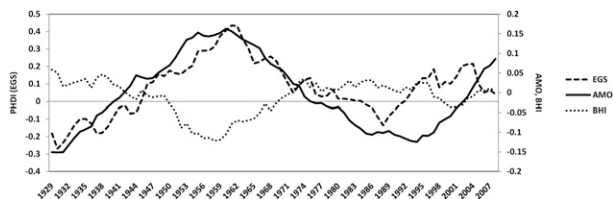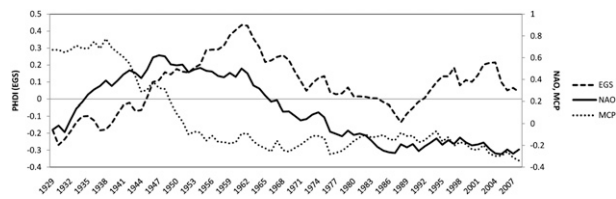
FIG. 4. As in Fig. 2, but in the EGS.

FIG. 5. As in Fig. 3, but in the EGS.

displacement of the Bermuda high, and reduced central pressure in the anticyclone. This implies weaker southerly airflow with moisture advection diverted around the western flank of the Bermuda high west of the SEUS and into the EGS, south Texas, and northern Mexico (e.g., Curtis 2008). These findings agree with Enfield et al. (2001) who documented a tendency for strong upper-level ridging over the SEUS during warm phases of the AMO. Additionally, previous work indicates the tendency for an anomalous midtroposphere trough of low pressure over the Atlantic off the coast of South Carolina during warm phases of the AMO, which may result from anomalous latent heating of the atmosphere due to increased precipitation in the tropical north Atlantic (Sutton and Hodson 2005). The anomalous northeasterly and northerly airflow in the northwest quadrant of this cyclone dominates the SEUS, effectively minimizing onshore low-level moisture transport (Sutton and Hodson 2005; Curtis 2008). The period from the late 1930s to the early 1960s, including the longest and most severe warm-season drought (1953–57) in the SEUS during the instrumental period, illustrates the effects of these conditions (e.g., J. T. Ortegren 2008, unpublished manuscript).

Because the AMO exhibits most of the memory contained in Atlantic basin climate oscillations (e.g., Mo et al. 2009), predictability of multidecadal drought patterns in the SEUS and EGS likely depends on predictability in SST fluctuations, specifically regarding the causal mechanisms behind phase changes in the AMO. Feedbacks between ocean and atmosphere and between the tropics and extratropics may help explain these phase changes. When MCP is reduced and the Bermuda high is located west of its mean position (i.e., AMO+), northward heat transport by both atmosphere and ocean is reduced, as southerly airflow in the west flank of the Bermuda high (which drives the North Atlantic gyre) is both weaker than average and displaced well inland over the SEUS. Concurrently, warm SSTs in the tropical North Atlantic (AMO+) lead to a steeper meridional temperature gradient and stronger midlatitude westerlies. Under these circumstances, the combined reduction in poleward heat transport and enhanced evaporation over the North Atlantic lead (slowly) to reduced extratropical SSTs and the formation of dense, cold water in the far

North Atlantic. Cold water parcels then subside and travel equatorward, where they arrive and upwell along the thermocline in approximately 12 yr (Gu and Philander 1997), halting the warming of tropical SSTs and initiating the return to AMO−.

Under AMO−, MCP is enhanced and the Bermuda high is east of its mean position. Tropical SSTs are cool, the meridional temperature gradient is reduced, midlatitude westerlies weaken, and southerly flow on the western flank of the Bermuda high is stronger than average and centered near the mid-Atlantic coast. Enhanced poleward heat transport in the North Atlantic gyre and reduced evaporation warm the extratropical Atlantic, and convective deepwater formation in high latitude locations is reduced (Polyakov et al. 2005). The reduction in cold water parcels suggests that relatively warm water circulates from the northern Atlantic to the tropical Atlantic over approximately a decade, the cooling of tropical SSTs is reversed, and the return to AMO+ is initiated.

The MCP is significantly positively correlated with the NAO, indicating a tendency for increased central pressure in the Bermuda high during positive phases of the NAO. Also, the NAO modulates Atlantic SSTs in that positive NAO phases are associated with strong midlatitude westerlies, increased meridional heat transport, and evaporative cooling of the Atlantic in middle and high latitudes (Marshall et al. 2001). However, climate impacts on land related to the NAO are largely operative in the winter, and the NAO typically oscillates at the decadal and subdecadal time scales as opposed to the multidecadal time scales we analyzed (Greatbatch 2000). The relationship between low-frequency summer variability in the NAO and the MCP deserves further attention, specifically in the context that variability in both the NAO and the AMO appears to be linked at various time scales to relatively predictable ocean oscillations including tropical Atlantic SST variability, the global thermohaline circulation, and the meridional overturning circulation in the Atlantic (Marshall et al. 2001; Jungclaus et al. 2005; McCabe and Palecki 2006; Pohlmann et al. 2006). Future observational and modeling studies may improve our understanding of the physical or stochastic mechanisms behind these linkages.

FIG. 6. Temporal variability in the subtropical Atlantic mode of low-frequency ocean–atmosphere variability and the smoothed time series of the AMO index and the BHI. The subtropical Atlantic mode is closely associated with AMO variability, while the BHI is inversely associated with both the AMO and the subtropical Atlantic mode.
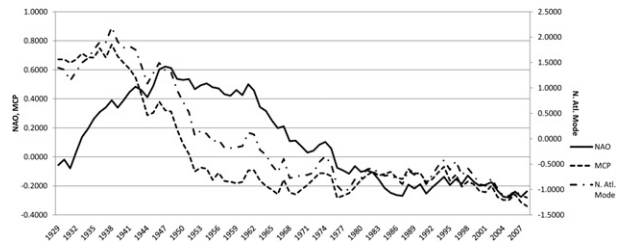

FIG. 7. The North Atlantic mode of ocean–atmosphere variability in comparison with the NAO and MCP indices. MCP indexes the strength of anticyclonic airflow around the Bermuda high.

e. Predictability assessment

To determine whether variability in the climate indices could be used to predict drought variability, we used linear regression (see section 3f). However, the colinearity of some of the climate indicators (e.g., AMO and BHI) precluded their use as predictors in traditional linear regression models. To express a majority of the variance in the climate indices in a smaller number of orthogonal (uncorrelated) variable dimensions, we ran rotated PCA on the 30-yr smoothed time series of all six climate indices for the common period 1900–2008 (e.g., Richman 1986). The three leading rotated PCs of ocean–atmosphere variability explained 95.16% of the variability in the climate index data. The rotated component loadings indicate that PC1 captures variability in the AMO and BHI, the second PC captures PDO and SOI variability (not shown), and PC3 captures primarily the MCP and NAO signals. Graphical evaluation supported these results (Figs. 6 and 7). Thus, we labeled the first PC of ocean–atmosphere variability the "subtropical Atlantic" mode, PC2 we called the "Pacific" mode, and PC3 the "North Atlantic" mode.

Neither the EGS nor the SEUS drought variability is significantly associated with the Pacific mode (PC2) of ocean–atmosphere variability. Low-frequency drought variability in the SEUS is significantly associated with both the subtropical Atlantic ($r = -0.782$) and the North Atlantic ($r = -0.558$) modes of synoptic variability. Low-frequency drought variability in the EGS is significantly associated with the same two modes ($r = 0.797$ and $r = -0.421$, respectively), but the correlation with the subtropical Atlantic component is of the opposite sign.

For the SEUS, the combined influences of these two modes explain 92.4% (R^2) of the variance in long-term warm-season moisture conditions (goodness-of-fit statistic $F = 467.3$, $p < 0.001$ for both predictors). Using the same regressor variables, we modeled low-frequency drought variability in the EGS as well. The model

explains 81.2% (R^2) of the low-frequency variability in this region ($F = 166.45$, $p < 0.001$ for both predictors). The standardized beta coefficients from the two models were similar but with opposite sign for the subtropical Atlantic mode.

Because of autocorrelation in the predictor variables (smoothed time series), we caution against comparing these model statistics with those that would result from using time series of interannual variability. The large-scale ocean–atmosphere features we analyzed are not hypothesized to enhance interannual predictability per se but have been shown to affect long-term patterns of summer moisture.

The model faithfully reproduced the low-frequency drought variability in both regions. For the SEUS, the Pearson correlation coefficient between predicted and observed series is 0.883 ($p < 0.001$). The RE statistic for the estimates is 0.564. Any positive value of the RE statistic is a robust indication that the model reliably replicates the observed variability in the time series and that the model substantially outperforms climatology or persistence (e.g., long-term mean) as a predictor (Fritts 1976). For the EGS, the correlation between model estimates and independent observed data is 0.634 ($p < 0.001$; RE = 0.223).

These findings suggest that low-frequency warm-season drought variability in the SEUS and EGS may be more predictable than currently recognized. The summer average conditions of the AMO, BHI, and MCP for the previous 30 years explain a substantial portion of the variability in warm-season drought conditions in both regions.

5. Conclusions

We identified nine distinct regions of warm-season drought variability in the conterminous United States during 1895–2009. We conclude that the EGS and SEUS regions are the least prone to long, severe droughts and that these regions may need to be assessed differently than the rest of the conterminous United States in terms of water resource management and drought preparation.

Multidecadal drought variability is evident in both regions, with 25–40-yr periods exhibiting above-average warm-season moisture followed by periods of similar length in which warm-season moisture is below the long-term mean.

We indexed the summer mean central pressure and the location of the western flank of the Bermuda high for the period 1895–2009 and identified associations between these two features and the AMO. The principal modes of ocean–atmosphere variability impacting low-frequency warm-season moisture conditions in the study area are the AMO–BHI and the MCP–NAO. Combined, the variability in these features explains >80% of the long-term drought variability in both regions. This indicates the possibility for improved baseline information used in decadal-scale drought forecasts based on knowledge of prior conditions and on monitoring of slow changes in subtropical Atlantic SSTs. Additionally, these relationships may enhance the design and/or input quality of global climate models aimed at multidecadal forecasts under various greenhouse gas scenarios. The potential for enhanced long-term climate forecasting emphasizes the importance of improved SST data monitoring throughout the Atlantic Basin, as the AMO appears to be a major contributor to low-frequency drought variability in the study areas. Water resource managers and water-intensive industries in the SEUS and EGS regions could benefit from the evidence indicating the strong cyclical (and typically out of phase) nature of warm-season moisture conditions in the two regions and from the evidence suggesting that coupled behavior in the AMO and BHI is the main driver of low-frequency drought variability.

REFERENCES

Acker, J. C., and P. T. Soulé, 1995: Temporal characteristics of Pennsylvania snowfall, 1950–1951 through 1989–1990. *Phys. Geogr.,* **16,** 188–204.

Anchukaitis, K. J., M. N. Evans, A. Kaplan, E. A. Vaganov, M. K. Hughes, H. D. Grissino-Mayer, and M. A. Cane, 2006: Forward modeling of regional scale tree-ring patterns in the southeastern United States and the recent influence of summer drought. *Geophys. Res. Lett.,* **33,** L04705, doi:10.1029/2005GL025050.

Cook, E. R., and P. J. Krusic, 2004: North American summer PDSI reconstructions. IGBP PAGES/World Data Center for Paleoclimatology Data Contribution Series No. 2004-045, NOAA/NGDC Paleoclimatology Program, 24 pp.

Cordery, I., and M. McCall, 2000: A model for forecasting drought from teleconnections. *Water Resour. Res.,* **36,** 763–768.

Curtis, S., 2008: The Atlantic multidecadal oscillation and extreme daily precipitation over the United States and Mexico during the hurricane season. *Climate Dyn.,* **30,** 343–351.

Davis, R. E., B. P. Hayden, D. A. Gay, W. L. Phillips, and G. V. Jones, 1997: The North Atlantic subtropical anticyclone. *J. Climate,* **10,** 728–744.

Diem, J. E., 2006: Synoptic-scale controls of summer precipitation in the southeastern United States. *J. Climate,* **19,** 613–621.

Enfield, D. B., A. M. Mestas-Nuñez, and P. J. Trimble, 2001: The Atlantic multidecadal oscillation and its relation to rainfall and river flows in the continental U.S. *Geophys. Res. Lett.,* **28,** 2077–2080.

Fritts, H. C., 1976: *Tree Rings and Climate.* Academic Press, 567 pp.

Greatbatch, R. J., 2000: The North Atlantic Oscillation. *Stochastic Environ. Res. Risk.,* **14,** 213–242.

Gu, D., and S. G. H. Philander, 1997: Interdecadal climate fluctuations that depend on exchanges between the tropics and extratropics. *Science,* **275,** 805–807.

Hayes, M. J., M. D. Svoboda, C. L. Knutson, and D. A. Wilhite, 2004: Estimating the economic impacts of drought. Preprints, *14th Conf. on Applied Climatalogy and 15th Symp. on Global Change and Climate Variations,* Lincoln, NE, Amer. Meteor. Soc., J2.6.

Henderson, K. G., and A. J. Vega, 1996: Regional precipitation variability in the southern United States. *Phys. Geogr.,* **17,** 93–112.

Herweijer, C., R. Seager, E. R. Cook, and J. Emile-Geay, 2007: North American droughts of the last millennium from a gridded network of tree-ring data. *J. Climate,* **20,** 1353–1376.

Hoerling, M., and A. Kumar, 2003: The perfect ocean for drought. *Science,* **299,** 691–694.

Horel, J. D., 1981: A rotated principal components analysis of the interannual variability of the Northern Hemisphere 500-mb height field. *Mon. Wea. Rev.,* **109,** 2080–2092.

Jungclaus, J. H., H. Haak, M. Latif, and U. Mikolajewicz, 2005: Arctic–North Atlantic interactions and multidecadal variability of the meridional overturning circulation. *J. Climate,* **18,** 4013–4031.

Kangas, R. S., and T. J. Brown, 2007: Characteristics of U.S. drought and pluvials from a high-resolution spatial dataset. *Int. J. Climatol.,* **27,** 1303–1325.

Katz, R. W., M. B. Parlange, and C. Tebaldi, 2003: Stochastic modeling of the effects of large-scale circulation on daily weather in the southeastern U.S. *Climatic Change,* **60,** 189–216.

Keim, B. D., 1997: Preliminary analysis of the temporal patterns of heavy rainfall across the southeastern United States. *Prof. Geogr.,* **49,** 94–104.

Knapp, P. A., H. D. Grissino-Mayer, and P. T. Soulé, 2002: Climatic regionalization and the spatio-temporal occurrence of extreme single-year drought events (1500–1998) in the interior Pacific Northwest, USA. *Quat. Res.,* **58,** 226–233.

Knight, J. R., C. K. Folland, and A. A. Scaife, 2006: Climate impacts of the Atlantic multidecadal oscillation. *Geophys. Res. Lett.,* **33,** L17706, doi:10.1029/2006GL026242.

Marshall, J., and Coauthors, 2001: North Atlantic climate variability: Phenomena, impacts, and mechanisms. *Int. J. Climatol.,* **21,** 1863–1898.

McCabe, G. J., and M. A. Palecki, 2006: Multidecadal climate variability of global lands and oceans. *Int. J. Climatol.,* **26,** 849–865.

——, ——, and J. L. Betancourt, 2004: Pacific and Atlantic Ocean influences on multidecadal drought frequency in the United States. *Proc. Natl. Acad. Sci. USA,* **101,** 4136–4141.

Mo, K. C., J. E. Schemm, and S. H. Yoo, 2009: Influence of ENSO and the Atlantic multidecadal oscillation on drought over the United States. *J. Climate,* **22,** 5962–5982.

Palmer, W. C., 1965: Meteorological drought. U.S. Weather Bureau Research Paper 45, U.S. Government Printing Office, 58 pp.

Pohlmann, H., F. Sienz, and M. Latif, 2006: Influence of the multidecadal Atlantic overturning circulation variability on European climate. *J. Climate,* **19,** 6062–6067.

Polyakov, I. V., U. S. Bhatt, H. L. Simmons, D. Walsh, J. E. Walsh, and X. Zhang, 2005: Multidecadal variability of North Atlantic temperature and salinity during the twentieth century. *J. Climate,* **18,** 4562–4581.

Richman, M. B., 1986: Rotation of principal components. *J. Climatol.,* **6,** 293–335.

Rogers, J. C., and J. S. M. Coleman, 2003: Interactions between the Atlantic multidecadal oscillation, El Niño/La Niña, and the PNA in winter Mississippi Valley stream flow. *Geophys. Res. Lett.,* **30,** 1518, doi:10.1029/2003GL017216.

Sahsamanoglou, H. S., 1990: A contribution to the study of action centres in the North Atlantic. *Int. J. Climatol.,* **10,** 247–261.

Schubert, S., M. Suarez, P. Pegion, R. Koster, and J. Bachmeister, 2004: Causes of long-term drought in the U.S. Great Plains. *J. Climate,* **17,** 485–503.

Seager, R., Y. Kushnir, C. Herweijer, N. Naik, and J. Velez, 2005: Modeling of tropical forcing of persistent droughts and pluvials over western North America, 1856–2000. *J. Climate,* **18,** 4065–4088.

——, A. Tzanova, and J. Nakamura, 2009: Drought in the southeastern United States: Causes, variability over the last millennium, and the potential for future hydroclimatic change. *J. Climate,* **22,** 5021–5045.

Soulé, P. T., 1992: Spatial patterns of drought frequency and duration in the contiguous U.S.A. based on multiple drought event definitions. *Int. J. Climatol.,* **12,** 11–24.

Stahle, D. W., and M. K. Cleaveland, 1988: Texas drought history reconstructed and analyzed from 1698 to 1980. *J. Climate,* **1,** 59–74.

——, and ——, 1992: Reconstruction and analysis of spring rainfall over the southeastern U.S. for the past 1000 years. *Bull. Amer. Meteor. Soc.,* **73,** 1947–1961.

——, and ——, 1994: Tree-ring reconstructed rainfall over the southeastern U.S.A. during the medieval warm period and little ice age. *Climatic Change,* **26,** 199–212.

——, ——, and J. G. Hehr, 1988: North Carolina climate changes reconstructed from tree rings: A.D. 372 to 1985. *Science,* **420,** 1517–1520.

——, D. B. Blanton, M. D. Therrell, and D. A. Gay, 1998: The Lost Colony and Jamestown droughts. *Science,* **280,** 564–567.

——, F. K. Fye, E. R. Cook, and R. D. Griffin, 2007: Tree-ring reconstructed megadroughts over North America since A.D. 1300. *Climatic Change,* **83,** 133–149.

Sutton, R. T., and D. L. R. Hodson, 2005: Atlantic Ocean forcing of North American and European summer climate. *Science,* **309,** 115–118.

Timilsena, J., and T. Piechota, 2008: Regionalization and reconstruction of snow water equivalent in the upper Colorado River basin. *J. Hydrol.,* **352,** 94–106.

Trenberth, K. E., G. W. Branstator, and P. A. Arkin, 1988: Origins of the 1988 North American drought. *Science,* **242,** 1640–1645.